Josephson effect in SS'IS'S tunnel structures

A. A. Golubov, M. A. Gurvich, M. Yu. Kupriyanov, and S. V. Polonskiĭ

Nuclear Physics Research Institute, Moscow
(Submitted 17 December 1992)
Zh. Eksp. Teor. Fiz. **103**, 1851–1868 (May 1993)

Within the framework of the Usadel equations we analyze the proximity effect at the interface of two superconducting metals in the case where the thickness d of one metal (S') is assumed much smaller than the coherence length ξ^* of that metal. We use numerical methods to calculate the density of states at the SS' interface, the gap Δ_g in the elementary-excitation spectrum, and the values of the order parameters Δ_s and Δ_n in the S and S' superconductors. We show that the temperature dependences of these quantities are determined by the suppression parameter $\gamma_M=\rho_s\xi_s^*d/\rho\xi^{*2}$ and the critical temperature ratio T_c^*/T_c and generally do not coincide. The results are used to calculate the temperature dependences of the critical current and current-voltage characteristics of high-capacitance SS'IS'S tunneling junctions. We examine the way in which these characteristics vary with the parameter γ_M and the T_c^*/T_c ratio and show that the critical current in NbN/Nb/Al/AlO_x/Al/Nb/NbN structures may amount to 90% and 30% of the maximum possible value in the liquid-helium temperature range and near T_c, respectively, while a study of the features of current-voltage characteristics may yield additional information about the properties of the Nb/Al boundary.

INTRODUCTION

The substantial achievements in the field of superconducting electronics (the design of highly sensitive magnetometers and related devices, receivers of electromagnetic radiation, and devices using fast single-quantum logic) are due in many respects to the emergence of the so-called niobium-aluminum technology of manufacturing Josephson Nb–AlO_x–Nb tunnel junctions. At a certain stage of manufacturing (with the aim of forming an insulator layer) this technology provides for oxidation of a thin layer of aluminum previously deposited on niobium. As a rule, however, there is a residue layer of aluminum left between the superconductor and the insulator layer. More than that, in junctions used as detectors of x rays such a residual layer is specially reproduced on both sides of the insulator layer.[1–4] Since aluminum is a superconductor with a transition temperature $T_c^* \approx 2.7$ K, the resulting junctions are of the SS'IS or SS'IS'S type.

Further development of this avenue of research is the change from Nb to superconducting electrodes with a higher transition temperature, for instance NbN. But in contrast to Nb, the morphology of the NbN surface is move complicated, and the surface's wettability is substantially lower than that of aluminum. Hence, simple transference of the manufacturing technology of Nb–AlO_x–Nb structures to NbN–AlO_x–NbN junctions has not led to success. One solution to the emerging problems is to use a thin layer of Nb as a buffer between NbN and Al, that is, manufacturing NbN–(Nb–AlO_x–Nb)–NbN junctions. Since the coherence length of Nb is much shorter than that of Al, for layers of these metals of roughly the same thickness the properties of the junctions are chiefly determined by the proximity effect at the NbN–Nb interfaces, that is, are close to the characteristics of structures of the SS'IS'S type.

The earlier theoretical studies of the properties of Nb–AlO_x–Nb tunnel junctions used the model of an SNINS junction,[5,6] which assumes that the N-metal is truly normal, that is, has $T_c^*=0$. The model provides a qualitative description of the main features of Nb–AlO_x–Nb junctions: the knee-like structure of the current-voltage characteristics, the suppressed critical-current values I_c (in comparison with those that follow from the microscopic theory of SIS structures; see Refs. 7 and 8), and the effective gap Δ_g in the elementary-excitation spectrum. The model, however, yields essentially understated quantitative estimates, especially for NbN–(Nb–AlO_x–Nb)NbN Josephson junctions, in which the transition temperature T_c^* usually differs from zero considerably.

The goal of the present paper is to build a theory of SS'IS'S tunneling Josephson junctions with spatially inhomogeneous superconducting properties of the SS'-electrodes, a theory that allows for a finite transition temperature of the S' layers.

1. JUNCTION MODEL

We assume that at least one of the electrodes of the SIS tunneling junction is an SS' sandwich, with the thickness d of the S'-layer obeying the following condition:

$$d \ll \xi^*, \tag{1}$$

where $\xi^*=(D/2\pi T_c)^{1/2}$ is the effective coherence length in the S'-metal, and T_c the transition temperature of the massive superconductor. We also assume that the S and S' materials meet the "dirty" limit conditions and that the

 1063-7761/93/050915-09$10.00

transverse dimensions of the tunneling junction, W, satisfy the condition $W<\lambda_J$, where λ_J is the Josephson penetration depth, so that all quantities can be assumed to depend only on one coordinate x along the normal to the material's surface. Below we restrict our discussion to the case most important from the practical viewpoint, namely, the case of fairly thick superconducting electrodes, that is, we do not allow for the decrease in the transition temperature of the SS'-electrode in comparison with the T_c of the massive S material.

The low junction transparency makes it possible, when studying the junction properties, to ignore the suppression of the superconductivity of the electrodes by the current flowing in them and to employ the formulas of classical tunnel theory,[7,8] according to which the current is determined by the retarded Green functions in the electrodes, $F(\varepsilon)$ and $G(\varepsilon)$. For instance, for large values of the McCumber–Stewart parameter, $\beta\gg 1$, when the voltage across the junction remains practically constant, the current through the junction is determined by the relation

$$I=\operatorname{Re} J_p(V)\sin\varphi+\operatorname{Im} J_p(V)\cos\varphi+\operatorname{Im} J_q(V),$$
$$\varphi=2eVt+\varphi_0, \tag{2}$$

where φ is the difference in the phases of the electrode's order parameter,

$$\operatorname{Re} J_p(V)=\frac{\sigma_N}{2e}\int d\varepsilon \operatorname{th}\left[\frac{\varepsilon}{2T}\right][\operatorname{Im} F_1(\varepsilon)\operatorname{Re} F_2(\varepsilon+eV)$$
$$+\operatorname{Re} F_1(\varepsilon+eV)\operatorname{Im} F_2(\varepsilon)]$$

the amplitude of the Josephson supercurrent,

$$\operatorname{Im} J_q(V)=\frac{\sigma_N}{2e}\int d\varepsilon\left[\operatorname{th}\frac{\varepsilon+eV}{2T}-\operatorname{th}\frac{\varepsilon}{2T}\right]$$
$$\times\operatorname{Im} F_1(\varepsilon+eV)\operatorname{Im} F_2(\varepsilon) \tag{3}$$

the amplitude of the dissipative component of the current caused by the interference of pairs and quasiparticles, and

$$\operatorname{Im} J_q(V)=\frac{\sigma_N}{2e}\int d\varepsilon\left[\operatorname{th}\frac{\varepsilon+eV}{2T}-\operatorname{th}\frac{\varepsilon}{2T}\right]$$
$$\times\operatorname{Re} G_1(\varepsilon)\operatorname{Re} G_2(\varepsilon+eV) \tag{4}$$

determines the quasiparticle current. Here the subscripts 1 and 2 refer to the left and right electrodes, respectively, and σ_N is the conductivity per unit surface area of the junction.

When calculating the current (2) we can employ condition (1) and assume that the functions $\operatorname{Re}G(\varepsilon)$, $\operatorname{Re}F(\varepsilon)$, and $\operatorname{Im}F(\varepsilon)$ are equal to their values at the SS' interface, that is, ignore the unlikely processes of electrons tunneling from the bulk of the SS'-electrode.

As noted in Ref. 5, the problem of determining the functions $\operatorname{Re}G(\varepsilon)$, $\operatorname{Re}F(\varepsilon)$, and $\operatorname{Im}F(\varepsilon)$ in Eqs. (2)–(4) must be solved in two stages. In the first the spatial dependence of the order parameter $\Delta(x)$ in the compound SS'-electrode is determined by solving the Usadel equations.[9] Then, using this function, we must solve the analytically continued (by replacing ω with $-i\varepsilon$) Usadel equations.

2. THE PROXIMITY EFFECT IN THE SS' SANDWICH

We place the origin of coordinates in the SS' interface and direct the x axis perpendicularly to this interface. Then in the gauge in which the vector potential is zero the Usadel equations describing the properties of these metals can be represented in the form (the region where $x\geqslant 0$ is occupied by the massive superconductor (S) and the region where $-d\leqslant x\leqslant 0$ by the S metal):

$$\left.\begin{aligned}&\Phi_s=\Delta_s+(\xi_s^*)^2\frac{\pi T_c}{\omega G_s}[G_s^2\Phi_s']',\quad G_s=\frac{\omega}{(\omega^2+\Phi_s^2)^{1/2}}\\&\Delta_s\ln\{T/T_c\}+2\pi T\sum_{\omega>0}\{(\Delta_s-\Phi_s G_s)/\omega\}=0\end{aligned}\right\}x\geqslant 0, \tag{5}$$

$$\left.\begin{aligned}&\Phi=\Delta_n+(\xi^*)^2\frac{\pi T_c}{\omega G}[G^2\Phi']',\quad G=\frac{\omega}{(\omega^2+\Phi^2)^{1/2}}\\&\Delta_n\ln\{T/T_c^*\}+2\pi T\sum_{\omega>0}\{(\Delta_n-\Phi G)/\omega\}=0\end{aligned}\right\}-d\leqslant x\leqslant 0. \tag{6}$$

Here Φ and Φ_s, and Δ_n and Δ_s are modified Usadel functions and the order parameters in the S and S' materials, respectively, ω is the Matsubara frequency, and a prime denotes a derivative with respect to coordinate x.

Equations (5) and (6) must be supplemented by boundary conditions in the bulk of the S-electrode,

$$\Phi_s(\infty)=\Delta_s(\infty)=\Delta(T), \tag{7}$$

and also at the interface of the S' metal and the massive superconductor[10] (in what follows the transparency of this interface is assumed to be close to unity),

$$\Phi(0)=\Phi_s(0),\quad \xi_s^*\Phi_s'(0)=\gamma\xi^*\Phi'(0),$$
$$\gamma=(\rho_s\xi_s^*)/(\rho\xi^*) \tag{8}$$

and at the interface of the S' metal and the insulator,

$$\Phi'(-d)=0. \tag{9}$$

Here $\Delta(T)$ is the absolute value of the order parameter of a homogeneous superconductor at a temperature T, and ρ and ρ_s are the conductivities of the S' and S metals, respectively.

In the limit of a thin S' layer, $d\ll\xi^*$, Eqs. (6) contain two characteristic frequencies, $\Omega_c\approx\pi T_c$ and $\Omega_d\approx\pi T_c\times(\xi^*/d)^2\gg\Omega_c$. In the frequency range $\omega\leqslant\Omega_d$ we ignore the nongradient terms in (6) in the first approximation in d/ξ^* and, allowing for (9), obtain

$$\Phi=A=\text{const},\quad \Delta_n=B=\text{const}. \tag{10}$$

Substituting (10) into (6), in the next approximation in d/ξ^* we obtain

$$\Phi=A+(A-B)\frac{(\omega^2+A^2)^{1/2}}{\pi T_c}\left[\frac{x^2+2dx}{2\xi^*}\right],\quad \omega\ll\Omega_d. \tag{11}$$

Since summation in the self-consistency equation (6) is convergent for $\omega>\Omega_d$, to find the relationship between the constants A and B we must know the behavior of the Φ_N functions at higher frequencies. We employ the fact

that for $\omega > \Omega_c$ the Usadel equations are linearized and, with Δ constant, they allow for an analytical solution of the form

$$\Phi = A + (A-B)\frac{\mathrm{ch}[\beta(x+d)/\xi^*]}{\mathrm{ch}[\beta d/\xi^*]}, \quad \beta = \left[\frac{\sqrt{\omega^2+A^2}}{\pi T_c}\right]^{1/2}, \tag{12}$$

which in the frequency range $\Omega_c \ll \omega \ll \Omega_d$ automatically transforms into Eq. (11). Substituting (12) into the self-consistency equation (6) and allowing for the fact that

$$2\pi T \sum_{\omega>0} \frac{\mathrm{ch}[\beta(x+d)/\xi^*]}{(\omega^2+A^2)^{1/2}\mathrm{ch}[\beta d/\xi^*]} \approx \ln\left[\frac{2\gamma^*\Omega_d}{\pi T}\right]$$

$$-2\pi T \sum_{\omega>0}\left[\frac{1}{\omega} - \frac{1}{(\omega^2+A^2)^{1/2}}\right],$$

where $\gamma^* = 1.78$ is Euler's constant, we arrive at the following relations:

$$B = A\left[\ln\left[\frac{2\gamma^*\Omega_d}{\pi T}\right] - \Sigma_1\right]\ln^{-1}\left[\frac{2\gamma^*\Omega_d}{\pi T}\right],$$

$$\Sigma_1 = 2\pi T \sum_{\omega>0}\left[\frac{1}{\omega} - \frac{1}{(\omega^2+A^2)^{1/2}}\right], \tag{13}$$

which makes it possible, provided Eq. (11) is taken into account, to write the boundary conditions (8) in a form closed with respect to Φ_s:

$$\xi_s^*\Phi_s'(0) = \gamma_{\mathrm{eff}}(\omega/\pi T_c)\Phi_s(0)/G_s(0),$$

$$\gamma_{\mathrm{eff}} = \gamma_M\left[\ln\left[\frac{T}{T_c'}\right] + \Sigma_1\right]\ln^{-1}\left[\frac{2\gamma^*\Omega_d}{\pi T_c^*}\right],$$

$$\gamma_M = \gamma\left(\frac{d}{\xi^*}\right), \tag{14}$$

thus reducing the problem to solving the Usadel equations in the superconductor. From (14) we see that the solution depends strongly on the magnitude of parameter γ_{eff}.

2.1. The approximation of small values of γ_{eff}

For fairly small values of γ_{eff} the boundary conditions (14) imply that

$$\xi_s^*\Phi_s'(0) = 0 \tag{15}$$

for $\omega \ll \Omega_\gamma = \pi T_c/\gamma_{\mathrm{eff}}$ in the zeroth approximation in γ_{eff}. Since the sum in the self-consistency equation (5) converges for frequencies $\Omega_c \ll \Omega_\gamma$, we can assume that both Δ_s and Φ_s in this approximation are independent of coordinate x:

$$\Phi_s(x) = \Delta_s(x) = A = \Delta(T), \quad \omega \ll \Omega_\gamma = \pi T_c/\gamma_{\mathrm{eff}}. \tag{16}$$

In the range of frequencies $\omega \approx \Omega_\gamma$ the Usadel equations (5) are linearized and are satisfied, if we allow for (14), by a solution of the form

$$\Phi_s(x) = \Delta(T)(1 - (\gamma_{\mathrm{eff}}\beta/(1+\gamma_{\mathrm{eff}}\beta))\exp\{-\beta x/\xi_s^*\}), \tag{17}$$

from which we have for $\Phi_s(0)$

$$\Phi_s(0) = \Delta(T)/(1+\gamma_{\mathrm{eff}}\beta). \tag{18}$$

Substituting (16) into (13) and (14), we arrive at a condition for the applicability of the approximation:

$$\gamma_{\mathrm{eff}} = \gamma_M \ln\left[\frac{T_c}{T_c^*}\right]\ln^{-1}\left[\frac{2\gamma^*\Omega_d}{\pi T_c^*}\right] \ll 1. \tag{19}$$

As $T_c^* \to 0$, the above inequality transforms into the one ($\gamma_M \ll 1$) established in Ref. 5 for SNINS junctions with a truly normal metal. We see that the closer T_c^* is to T_c and the smaller the thickness S′ of the layer, the less stringent are the requirements imposed on the suppression parameter γ_M.

2.2. The approximation of large values of γ_{eff}

In this approximation the boundary condition (14) in the range $\omega \gg \pi T_c/\gamma_{\mathrm{eff}}$ is reduced in the zeroth approximation in $\gamma_{\mathrm{eff}}^{-1}$ to the equality

$$\Phi_s(0) = 0. \tag{20}$$

The solution to Eq. (5) with the boundary conditions (7) and (20) was obtained in Ref. 10. There it was shown, among other things, that in the neighborhood of the SS′ interface ($0 < x < \xi_s^*$) the functions Φ_s are given by

$$\Phi_s = B(T)x/\xi_s^*,$$

$$B(T) = 2T_c(1-(T/T_c)^2)/(7\zeta(3))^{1/2}, \tag{21}$$

where $\zeta(3)$ is Riemann's zeta function. Substituting (21) into (14) in the next approximation in $\gamma_{\mathrm{eff}}^{-1}$, we get

$$B(T) = \gamma_M\Phi_s(0)\frac{\omega}{\pi T_c}\frac{\ln(T/T_c^*) + (7\zeta(3)/8)\Phi_s^2\pi^2T^2}{\ln(2\gamma^*\Omega_d/\pi T_c^*)}. \tag{22}$$

We see that at temperatures not too close to T_c^*,

$$\ln(T/T_c^*) \gg (\Phi_s(0)/\pi T)^2, \tag{23}$$

the values of the functions Φ_s(o) at the SS′ interface are proportional to $B(T)$:

$$\Phi_s(0) = B(T)\frac{\pi T_c \ln(2\gamma^*\Omega_d/\pi T_c^*)}{\omega\gamma_M\ln(T/T_c^*)} \propto (T_c - T). \tag{24}$$

For a condition opposite to (23), that is, at $T \approx T_c^*$, we have

$$\Phi_s(0) = \pi T_c\left[\frac{8T^2B(T)}{7\zeta(3)\omega T_c^2\gamma_M}\ln(2\gamma^*\Omega_d/\pi T_c^*)\right]^{1/3}$$

$$\propto (T_c - T)^{1/3}. \tag{25}$$

Formulas (24) and (25) are valid if $\Phi_s(0) \ll \pi T$, which for $T \approx T_c^*$ is reduced to the requirement that

$$\gamma_M \gg \ln(2\gamma^*\Omega_d/\pi T_c^*)[(T_c/T_c^*)^2 - 1], \tag{26}$$

and at $T \approx T_c$ can be written as

$$\gamma_M \gg \frac{\ln(2\gamma^*\Omega_d/\pi T_c^*)}{\ln(T_c/T_c^*)}\left[1 - \left(\frac{T}{T_c}\right)^2\right]. \tag{27}$$

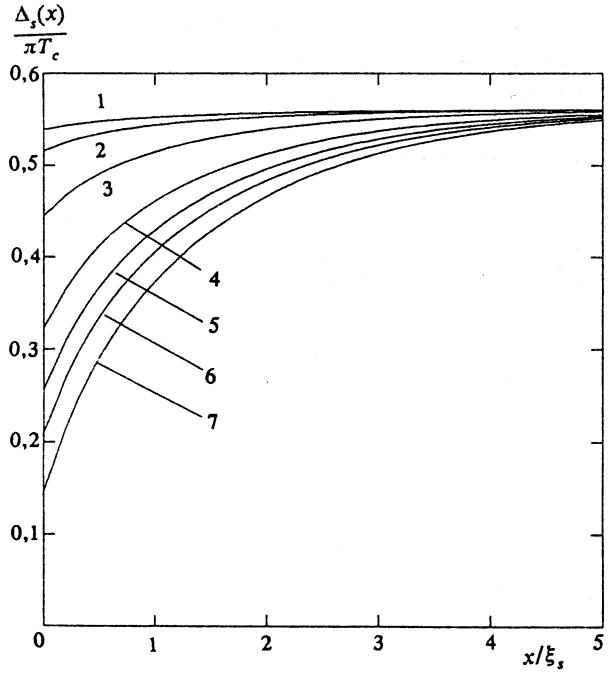

FIG. 1. The spatial dependence of the order parameter in the S region, $\Delta_s(x)$, at $\gamma_M=1$ for different values of T_c^*/T_c: 0.8, 0.5, 0.3, 0.1, 10^{-2}, 10^{-4}, and 0 (curves *1–7*, respectively).

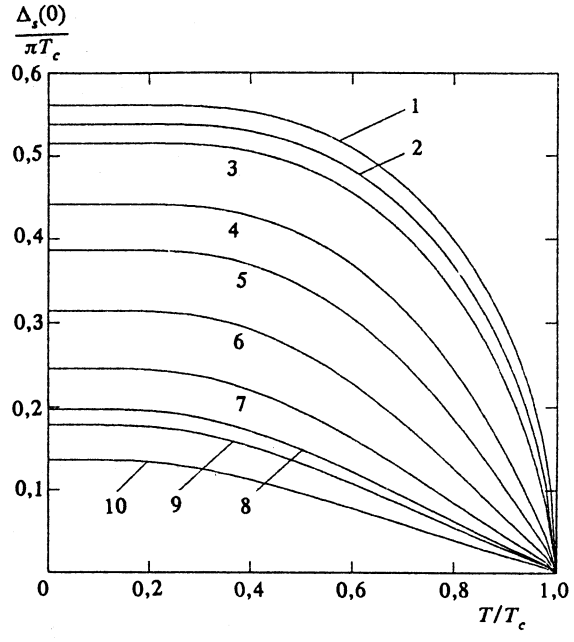

FIG. 2. The temperature dependences of the order parameter $\Delta_s(x=0)$ at the SS′ interface as $x\to+0$ and at $\gamma_M=1$, for different values of T_c^*/T_c: 1.0, 0.8, 0.5, 0.2, 0.1, 10^{-2}, 10^{-3}, 10^{-4}, 10^{-6}, and 0 (curves *1–10*, respectively.

The structure of formulas (24)–(27) implies that the values of the functions $\Phi_s(0)$ depend on the dependence between T and T^*, with

$$T^*=T_c^*+\frac{\ln(2\gamma^*\Omega_d/\pi T_c^*)}{\pi\gamma_M\ln(T_c/T_c^*)}\left(\left(\frac{T_c}{T_c^*}\right)^2-1\right). \qquad (28)$$

For $T\geqslant T^*$ the fact that the transition temperature of the S′ material is finite leads only to a slight decrease (in comparison to γ_M) in the absolute value of the suppression parameter γ_{eff}, which, as follows from (14), is given by the following relation:

$$\gamma_{\text{eff}}=\gamma_M\frac{\ln(T/T_c^*)}{\ln(2\gamma^*\Omega_d/\pi T_c^*)}. \qquad (29)$$

The temperature dependence of $\Phi_s(0)$ is determined by the function $B(T)$, that is, as in the SN sandwich, $\Phi_s(0)\propto(T_c-T)/\gamma_{\text{eff}}$.

At temperatures close to T^* there is a transition to weaker functional dependences of $\Phi_s(0)$ on T and γ_M determined in (25), $\Phi_s(0)\propto[T_c-T)/\gamma_{\text{eff}}]^{1/3}$, accompanied by a sharp increase in the absolute values of $\Phi_s(0)$.

2.3. Arbitrary values of γ_{eff}

For arbitrary temperatures and values of γ_M and T_c^*/T_c the system of equations (5), (7), and (14) was solved numerically. The results are depicted in Figs. 1–3.

Figure 1 shows the spatial variations of the order parameter in the S-electrode at $T=0.1T_c$ and $\gamma_M=1$. Curve *7* depicts the Δ_s vs x dependence calculated earlier in Ref. 5 while analyzing the proximity effect of a superconductor with a thin layer and a truly normal metal ($T_c^*=0$). Clearly, even a slight increase in T_c^*/T_c leads to a substantial increase in the absolute values of Δ, and in the case of a Nb/Al or NbN/Nb sandwich ($T_c^*/T_c\approx 0.2$–0.3) such an increase amounts to approximately 50%.

Figure 2 and 3 depict the temperature dependences of the order parameter at the SS′ interface, $\Delta_s(x=0)$, and in

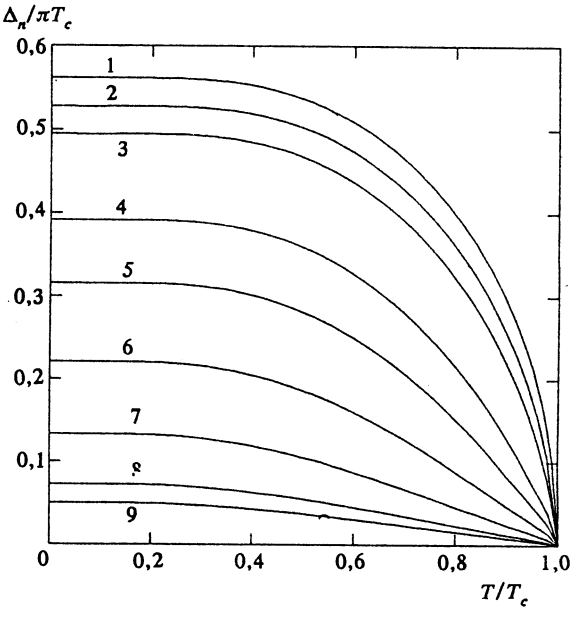

FIG. 3. The temperature dependences of the order parameter Δ_n in the S′ region at $\gamma_M=1$ for different values of T_c^*/T_c: 1.0, 0.8, 0.5, 0.2, 0.1, 10^{-2}, 10^{-3}, 10^{-4}, and 10^{-6} (curves *1–9*, respectively).

the S′ layer, Δ_n, at $\gamma_M=1$ and various values of T_c^*/T_c. We see that for arbitrary temperatures, too, the limiting transition in parameter T_c^*/T_c from S′ to the N metal proceeds very slowly, so that even for T_c^*/T_c as small as one part in a million the order parameter in the S′ region, Δ_n, is distinctly nonzero. Such behavior agrees fully with the logarithmic dependence of the effective suppression parameter γ_{eff} on T_c^*/T_c specified in (14).

3. STATIONARY PROPERTIES OF SS′IS′S AND SS′IS TUNNEL STRUCTURES

It has proved expedient to write the expression that follows from (2) for the critical current in a tunnel junction in the Matsubara representation:

$$\frac{eI_cR_N}{2\pi T_c}=\frac{T}{T_c}\sum_{\omega>0}\omega^{-2}\Phi_{s1}(0)G_{s1}(0)\Phi_{s2}(0)G_{s2}(0), \quad (30)$$

where, as before, subscripts 1 and 2 refer to the first and second electrodes.

In the limit of small values of γ_{eff}, from Eqs. (18) and (30) we arrive in the case of SS′IS′S junctions at the following temperature dependence of I_c:

$$\frac{eI_cR_N}{2\pi T_c}=\frac{T}{T_c}\sum_{\omega>0}\frac{\Delta^2(T)}{\omega^2(1+\gamma_{\text{eff}}\beta)^2+\Delta^2(T)}$$

$$\approx\frac{\Delta(T)}{4T_c}\text{th}\left[\frac{\Delta(T)}{2T}\right]$$

$$-\gamma_{\text{eff}}\frac{T}{T_c}\sum_{\omega>0}\frac{\omega^2\Delta^2(T)}{(\omega^2+\Delta^2(T))^{7/4}(\pi T_c)^{1/2}}. \quad (31)$$

In particular, at temperatures close to T_c Eq. (31) yields

$$\frac{eI_cR_N}{2\pi T_c}=\frac{\Delta^2(T)}{8T_c^2}[1-\gamma_{\text{eff}}(14\zeta(3)/\pi^2)], \quad (32)$$

while for $T\ll T_c$, if we go in (31) from summation to integration with respect to ω, we get

$$\frac{eI_cR_N}{2\pi T_c}=\frac{\Delta(0)}{4T_c}\left[1-\gamma_{\text{eff}}\left[\frac{\Delta(0)}{T_c}\right]^{1/2}\frac{1}{6\pi 2\sqrt{2}}\left\{\Gamma\left(\frac{1}{4}\right)\right\}^2\right], \quad (33)$$

with $\Gamma(1/4)\approx 3.626$ the gamma function.

For large values of the suppression parameter, in the $T_c^* < T < T^*$ range which is most interesting from the practical viewpoint, Eqs. (25) and (30) yield

$$\frac{eI_cR_N}{2\pi T_c}=\frac{4}{7\zeta(3)}\left[\frac{T_c}{T}\right]^{1/3}\left[\frac{2}{\pi\gamma_M}\ln\frac{2\gamma^*\Omega_d}{\pi T_c^*}\left(1-\frac{T}{T_c}\right)\right]^{2/3}$$

$$\times\sum_{n=0}^{\infty}(2n+1)^{-8/3}. \quad (34)$$

For $T\geqslant T^*$, as in structures of the SNINS type, the critical current is proportional to $(T_c-T)^2$:

$$\frac{eI_cR_N}{2\pi T_c}=\frac{\pi^2}{96}\frac{T_c}{T}\left[\frac{B(T)}{T}\frac{\ln(2\gamma^*\Omega_d/\pi T_c^*)}{\gamma_M\ln(T/T_c^*)}\right]^2. \quad (35)$$

For arbitrary values of γ_{eff} and T_c^*/T_c, the temperature dependence of I_c was determined numerically. The results of calculations at $\gamma_M=1$ and $\gamma_M=0.1$ are depicted in Fig. 4. We see that the greater the values of the suppression parameter γ_M, the stronger the effect of the finiteness of the transition temperature of the S′ material on I_c. Here the critical current values calculated for $T\leqslant 0.4T_c$ with allowance for the fact that the transition temperature of Al is finite ($T_c^*/T_c\approx 0.2$–0.3) prove to be higher on the average by a factor of two ($\gamma_M=1$) and by a factor of 1.5 ($\gamma_M=0.1$) than those calculated earlier in Ref. 5 at $T_c^*=0$.

Similar calculations for SS′IS structures in the limit of

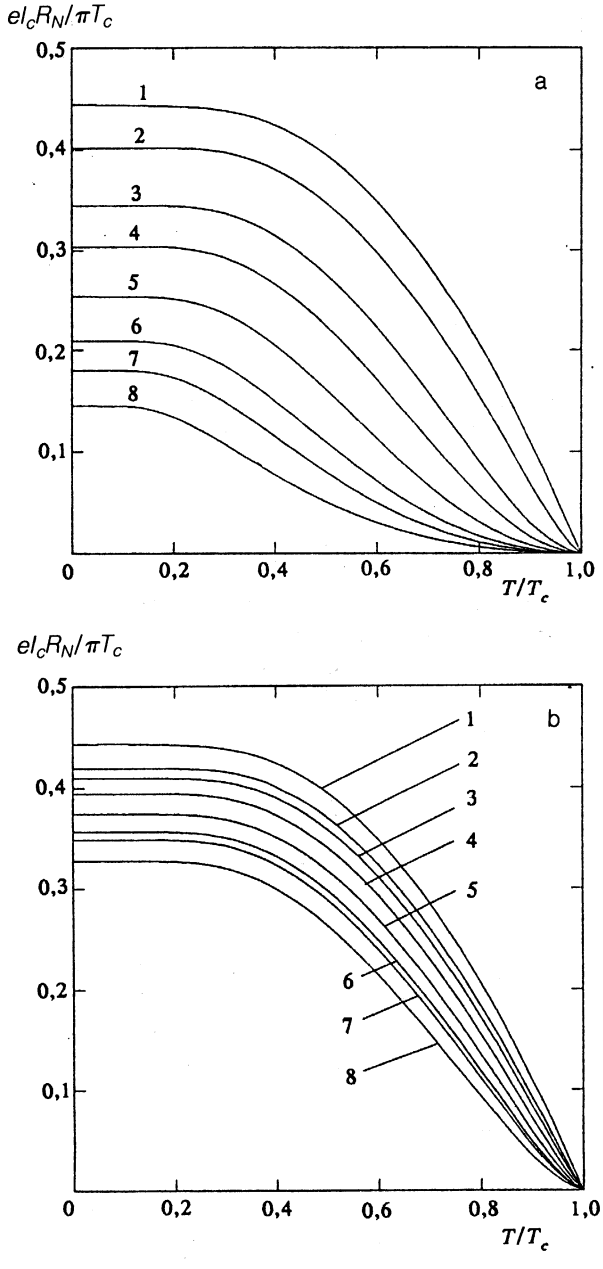

FIG. 4. The temperature dependences of the normalized critical current $I_ceR_N/\pi T_c$ in a symmetric SS′IS′S junction at (a) $\gamma_M=1$ and (b) $\gamma_M=0.1$ for different values of T_c^*/T_c: 1.0, 0.5, 0.2, 0.1, 10^{-2}, 10^{-3}, 10^{-4}, and 0 (curves *1–8*, respectively).

small values of γ_{eff} [Eq. (19)] lead to a temperature dependence of I_c of the form

$$\frac{eI_cR_N}{2\pi T_c}=\frac{T}{T_c}\sum_{\omega>0}\times\frac{\Delta^2(T)}{\{[\omega^2(1+\gamma_{\text{eff}}\beta)^2+\Delta^2(T)][\omega^2+\Delta^2(T)]\}^{1/2}}. \tag{36}$$

For large values of γ_{eff} and $T_c^*<T<T^*$, Eqs. (25) and (30) yield the following expression for the temperature dependence of I_c:

$$\frac{eI_cR_N}{2\pi T_c}=\frac{T}{T_c}\sum_{\omega>0}\frac{\pi T\Delta(T)}{\omega^{4/3}[\omega^2+\Delta^2(T)]^{1/2}}\times\left(\frac{8T^2B(T)}{7\zeta(3)T_c^2\gamma_M}\ln\frac{2\gamma^*\Omega_d}{\pi T_c^*}\right)^{1/3}, \tag{37}$$

from which it follows that $I_c\propto(T_c-T)^{5/6}$. As the temperature grows this dependence transforms for $T>T^*$ into one typical for SNIS junctions:

$$\frac{eI_cR_N}{2\pi T_c}=\frac{TB(T)\ln(2\gamma^*\Omega_d/\pi T_c^*)}{T_c\gamma_M\ln(T/T_c^*)}\times\sum_{\omega>0}\frac{\pi T_c\Delta(T)}{\omega^2[\omega^2+\Delta^2(T)]^{1/2}}\propto(T_c-T)^{3/2}. \tag{38}$$

Equations (36)–(38) imply that the finiteness of the transition temperature of the S′ material affects the critical current in junctions as strongly as it does in the case of SS′IS′S junctions.

4. NONSTATIONARY PROPERTIES OF SS′IS′S AND SS′IS TUNNEL STRUCTURES

According to Eqs. (2)–(4), to calculate the total current flowing through the tunnel junction we must know the density of states at the SS′ interface. In the region of small values of the suppression parameter γ_{eff} [Eq. (19)], using Eq. (18) we get

$$N(\varepsilon)=\text{Re}G_s(\omega\to-i\varepsilon)=\text{Re}\left\{\frac{-i\varepsilon(1+\gamma_{\text{eff}}\beta_\varepsilon)}{[\Delta^2(T)-\varepsilon^2(1+\gamma_{\text{eff}}\beta_\varepsilon)^2]^{1/2}}\right\}, \tag{39}$$

where $\beta_\varepsilon=[(\Delta^2(T)-\varepsilon^2)^{1/2}/\pi T_c]^{1/2}$. Analysis of Eq. (39) shows that the density of states has two singularities, one at $\varepsilon=\Delta(T)$ and the other at

$$\varepsilon=\Delta(T)(1-\gamma_{\text{eff}}^{4/3}(\Delta(T)/\pi T_c)^{2/3}). \tag{40}$$

The first does not manifest itself strongly, that is, $N(\varepsilon)\to(\varepsilon^2-\Delta^2(T))^{1/8}$ as $\varepsilon\to\Delta(T)\pm0$, and vanishes completely in the next approximation in γ_{eff}. The position of the second singularity determines the size of the gap in the elementary-excitation spectrum.

For arbitrary values of T_c^*/T_c and γ_{eff} it has been found expedient to go over to new functions $\Phi_s=\omega\tan\theta$ and $G_s=\cos\theta$ and then replace ω by $-i\varepsilon$ in Eqs. (5) and the boundary conditions (7) and (14)

$$(\xi_s^{*2}\theta''+i\tilde{\varepsilon}\sin\theta+\tilde{\Delta}(x)\cos\theta=0, \tag{41a}$$

$$\theta(\infty)=\text{arctg}(i\tilde{\Delta}(T)/\tilde{\varepsilon}), \tag{41b}$$

$$\xi_s^*\theta'(0)=-i\tilde{\varepsilon}\gamma_{\text{eff}}(T)\sin\theta(0). \tag{41c}$$

Here $\tilde{\varepsilon}=\varepsilon/\pi T_c$ and $\tilde{\Delta}(x)=\Delta(x)/\pi T_c$, and the ω-independent functions $\Delta(x)$ and the quantity $\gamma_{\text{eff}}(T)$ defined in (14) were found earlier in the first stage of calculations when the proximity effect was analyzed.

The results of calculations at $T=0.1T_c$ and $\gamma_M=1$ are depicted in Fig. 5. Clearly, at $T_c^*=0$ (curve *1*) the singularity in the density of states is completely smeared. An increase in parameter T_c^*/T_c changes the shape of the curves. This is accompanied by a growth of the energy gap (Fig. 6) and by the emergence, starting at $T\approx0.2T_c$, of a pronounced singularity manifesting itself in the current–voltage characteristics of the junctions (Fig. 7a) as a knee-like structure, whose maximum span is attained at $T_c^*/T_c\approx0.5$. Further increase in parameter T_c^*/T_c is accompanied by suppression of this structure and a smooth transition to curve *9* corresponding to the current–voltage characteristics of a classical SIS tunneling junction.

For fairly small $\gamma_M=0.1$ the knee-like structure in the current–voltage characteristics (Fig. 7b) manifests itself already at $T_c^*=0$. Clearly, here an increase in T_c^*/T_c is accompanied by an increase in the effective gap voltage. The width of the singularity in the current–voltage characteristics decreases while the peak value remains practically unchanged. However, starting with $T_c^*/T_c\approx0.2$, the

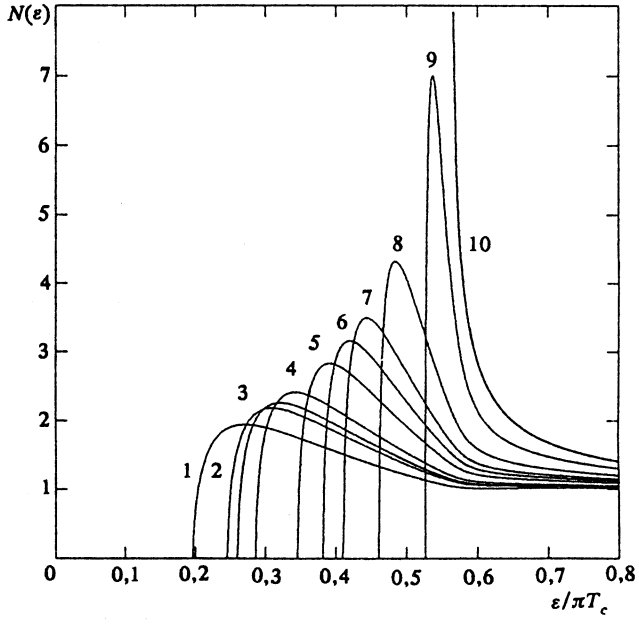

FIG. 5. The density of states at the SS′interface at $\gamma_M=1$ for different values of T_c^*/T_c: 0, 10^{-4}, 10^{-3}, 10^{-2}, 0.1, 0.2, 0.3, 0.5, 0.8, and 1 (curves *1–10*, respectively).

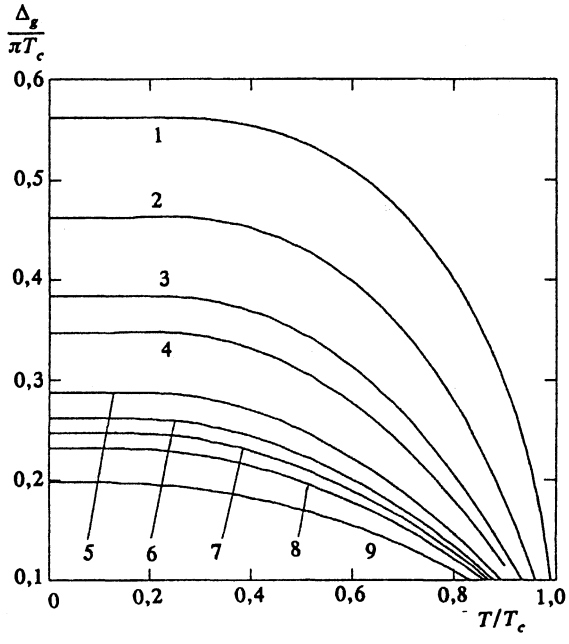

FIG. 6. The temperature dependences of the energy gap determined from N vs ε curves (Fig. 5) at $\gamma_M=1$ and for different values of T_c^*/T_c: 1.0, 0.5, 0.2, 0.1, 10^{-2}, 10^{-3}, 10^{-4}, 10^{-6}, and 0 (curves *1–9*, respectively).

peak value drops and a smooth transition to curve *9* corresponding to the current–voltage characteristic of a SIS junction is observed.

A simple comparison of the temperature dependences of the order parameter at the SS′ interface in the superconducting electrode, $\Delta_s(0)$ (Fig. 2), the order parameter in the S′ layer (Fig. 3), and the effective gap in the elementary-excitation spectrum (Fig. 6) points to a fairly strong difference between these values, and the larger the value of γ_M the greater the difference. This fact must be taken into account when analyzing the data on the size of the order parameter obtained by tunneling spectroscopy methods. The presence of factors leading to the spatial inhomogeneity of the order parameter in S-electrodes near the insulating layer results in the formation of singularities in the current–voltage characteristics at a voltage actually independent of the order parameter both at the SI interface, $\Delta_s(0)$, and in the bulk of the electrodes, $\Delta(T)$.

Figures 8 and 9 depict the variations in the current-voltage characteristics of SS′IS′S tunnel structures caused by variations in the suppression parameter γ_M at liquid-helium temperatures $T=4.2$ K for typical values of parameters of Nb/Al/AlO_x/Al/Nb and NbN/Nb/Al/AlO_x/Al/Nb/NbN junctions ($T_c^*=1.3$ K and $T_c=9.2$ K) and ($T_c^*=7$ K and $T_c=16$ K), respectively. Clearly, in both the first and second case at $\gamma_M\approx 1$ the knee-like structure is practically absent from the current-voltage characteristics. A decrease in γ_M is accompanied by the emergence of such a structure, with the peak value of the singularity attained at $\gamma_M\approx 0.2$. As the suppression parameter further decreases, the structure is suppressed. But even at $\gamma_M\approx 0.05$ it is still noticeable, and the transition to the current-

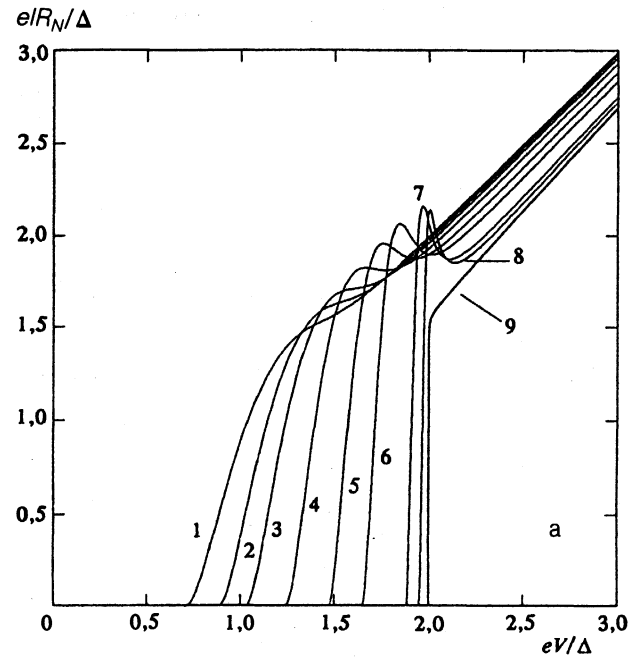

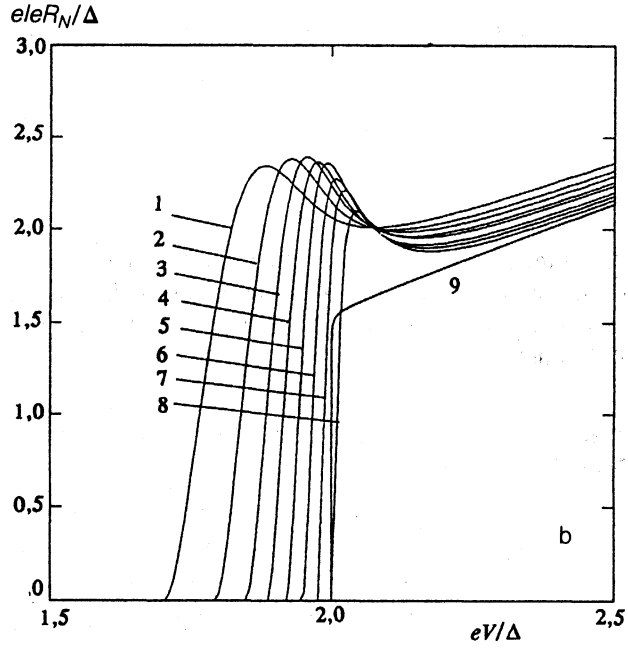

FIG. 7. Current-voltage characteristics of the SS′IS′S tunnel junction: (a) at $\gamma_M=1$ for $T_c^*/T_c=0$ (curve *1*), 10^{-4} (curve *2*), 10^{-2} (curve *3*), 0.1 (curve *4*), 0.3 (curve *5*), 0.5 (curve *6*), 0.8 (curve *7*), 0.9 (curve *8*), and 1.0 (curve *9*); and (b) at $\gamma_M=0.1$ for $T_c^*/T_c=0$ (curve *1*), 10^{-4} (curve *2*), 10^{-2} (curve *3*), 0.05 (curve *4*), 0.15 (curve *5*), 0.3 (curve *6*), 0.5 (curve *7*), 0.8 (curve *8*), and 1.0 (curve *9*).

voltage characteristic following from the classical theory of the tunneling effect (curve *9*) occurs when $\gamma_M\leqslant 0.01$.

5. CONCLUSION

The above calculations show that the finiteness of the transition temperature of the S′ material has the same

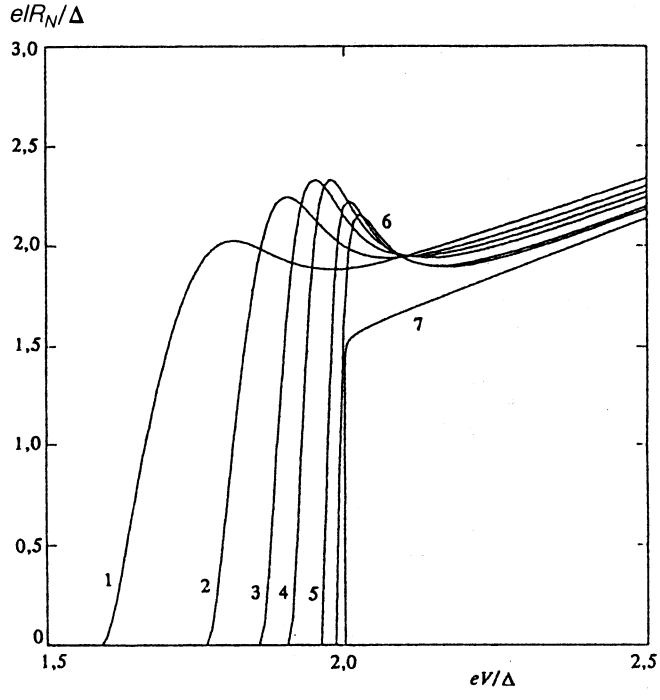

FIG. 8. Current-voltage characteristics of the SS'IS'S tunnel junction at $T_c^*=7$ K, $T_c=16$ K, and $T=4.2$ K (NbN/Nb/Al/AlO$_x$/Al/Nb/NbN) and different values of the suppression parameter $\gamma_M=1.0$ (curve *1*), 0.5 (curve *2*), 0.3 (curve *3*), 0.2 (curve *4*), 0.1 (curve *5*), 0.05 (curve *6*), and 0 (curve *7*).

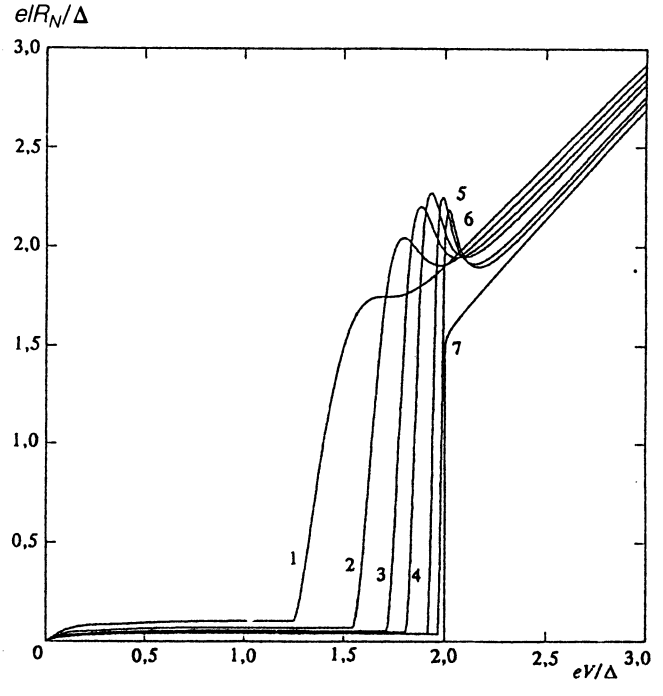

FIG. 9. Current-voltage characteristics of the SS'IS'S tunnel junction at $T_c^*=1.3$ K, $T_c=9.2$ K, and $T=4.2$ K (NbAl/AlO$_x$/AlNb) and different values of the suppression parameter $\gamma_M=1.0$ (curve *1*), 0.5 (curve *2*), 0.3 (curve *3*), 0.2 (curve *4*), 0.1 (curve *5*), 0.05 (curve *6*), and 0 (curve *7*).

strong effect on the characteristics of SS'IS'S tunnel structures as the suppression parameter γ_M and actually leads to an effective decrease of this parameter, in accordance with Eqs. (14) and (19).

For instance, for typical values of the parameters of the constituents of the NbN/Nb/Al/Al_2O_3/Al/Nb/NbN tunnel structure,

$$\begin{aligned}&\text{Nb—}\xi^*\approx 150\ \text{Å},\quad \rho\approx 10\ \mu\Omega\ \text{cm},\\ &T_c^*\approx 7\ \text{K},\quad d\approx 100\ \text{Å},\\ &\text{NbN—}\xi_S^*\approx 50\ \text{Å},\\ &\rho_S\approx 100\ \mu\Omega\ \text{cm},\quad T_c\approx 16\ \text{K},\end{aligned}\tag{42}$$

Eqs. (14) and (19) yield the following values for γ_M and γ_{eff}:

$$\gamma_M\approx 2,\quad \gamma_{\text{eff}}\approx 0.5.\tag{43}$$

The fact that the transition temperature of the S' material is finite, as we see, leads in the given situation to a sizable decrease of the effective suppression parameter. Equations (31) and (32) at $\gamma_{\text{eff}}\approx 0.5$ in the neighborhood of T_c and in the low-temperature range yield, respectively,

$$\frac{eI_cR_N}{2\pi T_c}\approx\begin{cases}0.3\Delta^2(T)/8T_c^2, & T\approx T_c,\\ 0.9\Delta(0)/4T_c, & T\leqslant 0.3T_c.\end{cases}\tag{44}$$

(Similar estimates for $T\ll T_c$ without allowing for the finiteness of the transition temperature of the S' layer yield values smaller by a factor of ten.)

Hence, in NbN/Nb/Al/Al_2O_3/Al/Nb/NbN junctions the product I_cR_N may, at least in the liquid-helium temperature range, reach values that differ only by 10–20% from the maximum possible one in NbN/I/Nb structures. The value of this product decreases as the temperature grows, and at $T\approx T_c$ the difference amounts to approximately 70%.

An aspect worth noting (see Fig. 8) is that in practice no knee-like singularity initiated by the proximity effect at the NbN/Nb interface should be observed in the current-voltage characteristics of NbN/Nb/Al/Al_2O_3/Al/Nb/NbN junctions. Experimental observation of such a singularity can be caused only by the proximity defect at the Nb/Al interface, and its study provides additional information about the suppression parameter at this interface. The parameter is small and has practically no effect on I_c.

Indeed, for typical values of the parameters of the materials comprising the Nb/Al/Al_2O_3/Al/Nb tunnel structure,

$$\begin{aligned}&\text{Nb—}\xi_S^*\approx 150\ \text{Å},\quad \rho_S\approx 10\ \mu\Omega\ \text{cm},\quad T_c\approx 9.2\ \text{K},\\ &\text{Al—}\xi^*\approx(\xi_0 l)^{1/2},\quad \rho\approx 1\ \mu\Omega\ \text{cm},\quad T_c^*\approx 1.3\ \text{K}.\end{aligned}\tag{45}$$

if we assume that the mean free path of electrons, l, in Al is of the order of the film thickness and $\xi_0\approx 10^4$ Å, Eqs. (14) and (19) yield the following values for γ_M and γ_{eff}:

$$\gamma_M\approx 0.1,\quad \gamma_{\text{eff}}\approx 0.05.\tag{46}$$

With values of γ_{eff} so small and in the liquid-helium temperature range, the correction to I_c that follows from Eq.

(33) proves to be of the order of one part in a hundred. However, the singularity in the current-voltage characteristics is still pronounced (see Fig. 9), which makes it possible to estimate γ_M for the Nb/Al interface knowing the experimental current-voltage characteristics.

In experimental realizations of the NbN/Nb/Al/Al_2O_3/Al/Nb/NbN tunneling junctions there is a possibility of nitrogen diffusion toward aluminum in the respective interfaces, which leads to formation of NbN/Al/Al_2O_3/Al/NbN structures. In the latter case, for typical values of the parameters of NbN and Al specified in (42) and (45) we get the following estimates for the suppression parameter:

$$\gamma_M \approx 0.5, \quad \gamma_{\text{eff}} \approx 0.2, \tag{47}$$

which are better than for the NbN/Nb interface. Hence, such diffusion does not lead to suppression of the critical current in the junctions.

It should also be noted that the appearance of fairly large values of the order parameter in the S′ layer already at $T_c^*/T_c \approx 10^5$ has a strong effect on the quasiparticle relaxation processes in SS′IS′S structures and should be taken into account when analyzing the operating conditions of SIS detectors of x rays.

[1] M. C. Gaidis, S. Friedrich, D. E. Prober *et al.*, IEEE Trans. Magn. **31**, No. 2 (1993).
[2] C. A. Mears, S. E. Labov, G. W. Morris *et al.*, IEEE Trans. Magn. **31**, No. 2 (1993).
[3] P. A. Narburton and M. G. Blamire, IEEE Trans. Magn. **31**, No. 2 (1993).
[4] E. P. Houwman, J. G. Gijsbertsen, J. Flokstra *et al.*, IEEE Trans. Magn. **31**, No. 2 (1993).
[5] A. A. Golubov and M. Yu. Kupriyanov, J. Low Temp. Phys. **70**, 83 (1988); A. A. Golubov and M. Yu. Kupriyanov, Zh. Eksp. Teor. Fiz. **96**, 1420 (1989) [Sov. Phys. JETP **69**, 805 (1989)].
[6] N. R. Werthemer, Phys. Rev. **147**, 255 (1966).
[7] A. I. Larkin and Yu. N. Ovchinnikov, Zh. Eksp. Teor. Fiz. **51**, 1535 (1966) [Sov. Phys. JEPT **24**, 1035 (1967)].
[8] K. Usadel, Phys. Rev. Lett. **25**, 560 (1970).
[9] M. Yu. Kupriyanov and V. F. Lukichev, Fiz. Nizk. Temp. **8**, 1045, 1982 [Sov. J. Low Temp. Phys. **8**, 526 (1982)].

Translated by Eugene Yankovsky
This article was translated in Russia, and it is reproduced here the way it was submitted by the translator, except for the stylistic changes by the Translation Editor.